

## MODELLING OF CONTACT GEOMETRY OF TOOL AND WORKPIECE IN GRINDING PROCESS WITH CROSSED AXES OF THE TOOL AND WORKPIECE WITH CIRCULAR PROFILE

Volodymyr KALCHENKO\*, Andrij YEROSHENKO\*, Sergiy BOYKO\*, Olga KALCHENKO\*

\*Mechanical Engineering Department, Chernihiv National University of Technology,  
95 Shevchenko street, 14035, Chernihiv, Ukraine

[vkalchenko74@gmail.com](mailto:vkalchenko74@gmail.com), [yeroshenkoam@gmail.com](mailto:yeroshenkoam@gmail.com), [svboyko.cstu@gmail.com](mailto:svboyko.cstu@gmail.com), [onkalchenko.2014@gmail.com](mailto:onkalchenko.2014@gmail.com)

*received 28 April 2020, revised 9 March 2021, accepted 15 March 2021*

**Abstract:** A general model is developed, and on its basis, there are special models formulated of the grinding process with crossed axes of the tool and workpiece with a profile in the form of a circle arc. A new method of control of the grinding process is proposed, which will provide processing by equidistant curves, and the amount of cutting of a circle equal to the allowance. This will increase the productivity and quality of grinding. The presented method of grinding implements the processing with the spatial contact line of the tool and workpiece. When the axes are crossed, the contact line is stretched, which leads to an increase of the contact area and, accordingly, to a decrease of the temperature in the processing area. This allows processing of workpieces with more productive cutting conditions.

**Key words:** circular arc, grinding, equidistant curves, cutting edge, abrasive surface, abrasive materials, crossed axes, abrasive wheel, heat stress, grinding performance

### 1. INTRODUCTION

Parts with high-precision surfaces and a profile in the form of arc of a circle, the final quality of which is ensured by abrasive machining, are widespread in modern mechanical engineering. Therefore, the amount of processing with abrasive tool is constantly growing in the total volume of the processing complexity.

One of the means of increasing the productivity and accuracy of grinding surfaces with a profile in the form of an arc of a circle is the development of grinding methods with intersecting axes of the tool and workpiece.

For grinding surfaces with a profile in the form of a circular arc angle of crossing axes, circle and part is a parameter that affects the productivity and quality of the grinding. It determines the distribution of the allowance and the amount of cutting the tool, the heat intensity of the grinding process, and the location and resistance of the forming section of the circle.

Therefore, for the effective processing of such surfaces, it is necessary to determine the optimal angles of the crossing axes of the workpiece and the tool (stationary or controlled), which provide an increase in productivity and accuracy of processing.

The main problem of grinding parts with a circular profile is the low resistance of the profile of abrasive tool, especially when grinding surfaces having high hardness and large machining allowances (Anderson et al., 2011; Kalpana et al., 2018). It is the crossing of the axes of the circle and the workpiece that determines the position of the forming section. Its combination with the normal along the coordinate of the processing makes it possible to compensate for the influence of the wear of the wheel profile on the accuracy of shaping, and increases the productivity and durability of the abrasive tool.

The development of new grinding methods with crossing axes of tool and parts with a profile in the form of a circular arc, and the

determination of rational angles axes crossing and tool profiling are urgent tasks of the grinding process, the solution of which will significantly increase productivity and machining accuracy, and ensure the abrasive wheel durability and the required quality of the machined surfaces.

Using the tool-oriented machining method, when the tool further alters the angular orientation with respect to the workpiece during cutting, it thereby eliminates the disadvantages of grinding with parallel axes of the tool and workpiece (Kalchenko et al., 2018). The removal of the allowance when grinding with the crossed axes is due to the transverse movement of the circle and its rotation relative to the straight line connecting the axis of rotation of the tool and the workpiece.

Thus, the purpose of the work is to develop a common model and, on its basis, special models of the grinding process with crossed axes of the tool and workpiece with circular profile.

### 2. THE GENERAL MODEL OF THE NOMINAL SURFACE OF THE WORKPIECE

In the works of other authors (Cong et al., 2018; Kacalak et al., 2018) there is a discussion concerning the development of a general model; to enable this development, it is necessary to solve the direct problem of the theory of formation. For this we need to mathematically describe complex surface detail, which is the general case all possible surfaces.

The surface of the workpiece is described by a spherical module. The sphericity of the module is caused by the presence of two independent angular parameters:  $\theta_w$  – is the angle of rotation around the axis of the workpiece rotation, and  $\varphi_w$  – angular coordinate of a circular profile, which may take a positive or negative value depending on the location of the starting point relative to the axial plane of the profile. All other model parame-

ters are functionally dependent on these two parameters.

The mathematical description of nominal workpiece surface can be performed by spherical module:

$$\bar{r}_w = S_{z_w \theta_w y_w \varphi_w y_p}^w \cdot e^{-4}, \quad (1)$$

where  $\bar{r}_w$  – is the radius vector of the points of the surface of a complex part;  $S_{z_w \theta_w y_w \varphi_w y_p}^w$  – spherical module a matrix of switching from the starting point in a coordinate system of the workpiece; and  $e^{-4} = (0,0,0,1)^T$  – radius vector of starting point (Kalchenko et al., 2018).

Spherical module of workpiece is a product of one-coordinate matrix (Kalchenko et al., 2018):

$$S_{z_w \theta_w y_w \varphi_w y_p}^w = M_3(z_w) M_6(\theta_w) \cdot M_2(y_w) \cdot M_4(\varphi_w) \cdot M_2(y_p), \quad (2)$$

where  $z_w$  – the axial coordinate of the profile offset which providing the screw surface;  $\theta_w$  – is the angle of rotation around the axis of the workpiece rotation;  $y_w$  – is the distance from the center of the profile to the axis of the workpiece rotation;  $\varphi_w$  – is the angle of rotation around the axis of  $Ox$ ;  $y_p = \rho_w$  – is the radius profile of the workpiece.

Thus, the matrices (Kalchenko et al., 2018), of which the module consists, have the following physical meaning:

$$M_2(y_p) = \begin{pmatrix} 1 & 0 & 0 & 0 \\ 0 & 1 & 0 & \pm y_p \\ 0 & 0 & 1 & 0 \\ 0 & 0 & 0 & 1 \end{pmatrix} - \text{the point displacement matrix}$$

along the axis  $O_w Y_w$ . Since the radius of curvature of the profile of a complex part varies depending on the axial coordinate  $z_w$ , which is functionally dependent on the angle of rotation  $\theta_w$ , the parameter  $y$  of the matrix  $M_2$  is a function of  $\theta_w$ :  $y_p = \rho_w(\theta_w)$ . In the particular case, when the radius of the workpiece profile does not change, the matrix parameter is converted to a constant. The sign ‘ $\pm$ ’ indicates that the radius can be set in different directions relative to the axis  $O_w Y_w$ . The sign ‘+’ indicates a concave outer or convex inner profile, and a ‘-’ indicates a convex outer or inner concave profile (Fig. 1).

$$M_4(\pm \varphi_w) = \begin{pmatrix} \cos \varphi_w & 0 & \sin \varphi_w & 0 \\ 0 & 1 & 0 & 0 \\ -\sin \varphi_w & 0 & \cos \varphi_w & 0 \\ 0 & 0 & 0 & 1 \end{pmatrix} - \text{matrix of generalized rotations of point about the axis } O_w X_w. \text{ The range of parameter change lies within the central angle } \xi.$$

The positive or negative values of the parameters  $\rho_w$  and  $\varphi_w$  are set depending on the direction of the axes of the selected coordinate system. Fig. 1 shows the directions of the axes of the coordinate system and the corresponding signs of the parameters  $\rho_w$  and  $\varphi_w$  for the various parts surfaces adopted in this work. For example, to describe the concave outer profile of the groove of the inner bearing ring  $\rho_w$  and  $\varphi_w$ , we take positive values (Fig. 1(a)), as well as for the convex outer profile of the belt pulley negative (Fig. 1(b)). Fig. 1 (a-d) shows surfaces with a central profile angle  $\xi = 180^\circ$ . Fig. 1(e) shows the general case of a concave outer surface for which the central angle is not equal to  $180^\circ$ .

$$M_2(y_w) = \begin{pmatrix} 1 & 0 & 0 & 0 \\ 0 & 1 & 0 & R_w \\ 0 & 0 & 1 & 0 \\ 0 & 0 & 0 & 1 \end{pmatrix} - \text{the point displacement matrix}$$

along the axis  $O_w Y_w$ , which sets the coordinate of the center of the

workpiece profile. For a complex part, this parameter, similar to  $y_p$ , is a function of the angle of rotation  $\theta_w$  and is converted to a constant value  $R_w$  for cylindrical parts.

$$M_6(\theta_w) = \begin{pmatrix} \cos \theta_w & -\sin \theta_w & 0 & 0 \\ \sin \theta_w & \cos \theta_w & 0 & 0 \\ 0 & 0 & 1 & 0 \\ 0 & 0 & 0 & 1 \end{pmatrix} - \text{a matrix of generalized rotations about the axis } O_w Z_w \text{ of the workpiece rotation.}$$

$$M_3(z_w) = \begin{pmatrix} 1 & 0 & 0 & 0 \\ 0 & 1 & 0 & 0 \\ 0 & 0 & 1 & z_w \\ 0 & 0 & 0 & 1 \end{pmatrix} - \text{axial displacement matrix of the profile.}$$

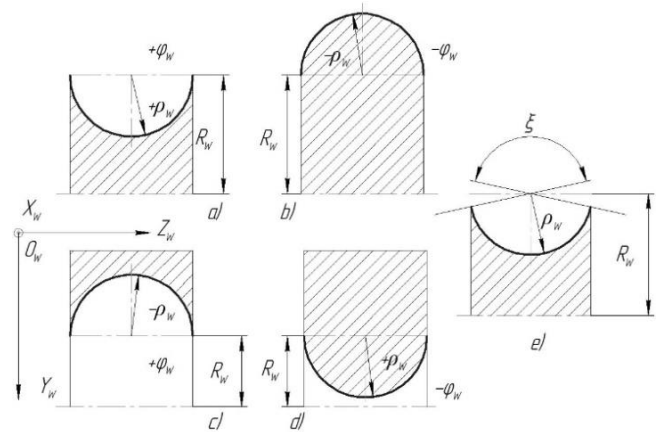


Fig. 1. Determining the type of workpiece profile

By rotating the profile of the workpiece around its axis of rotation with an angular coordinate  $\theta_w$  and giving it an axial offset with the coordinate  $z_w$ , we finally form the surface of the part. The axial coordinate of the screw surface  $z_w$  is a function of the angle of rotation of the workpiece:

$$z_w = \theta_w \cdot p \quad (3)$$

where  $p = \frac{S}{2\pi}$  – is screw motion parameter; and  $S$  – step screw surface.

Model (1) is general and describes all possible surfaces of parts with a circular profile. By taking the constants of individual model parameters, it becomes possible to describe the surfaces of specific parts. Consider the possible special models that can be obtained from the general model.

1. Screw surface with profile in the form of an arc of a circle. The screw surface is characterised by the dependence of the angular coordinate of the screw  $z_w$  on the angle of the workpiece rotation  $\theta_w$ , the constancy of the distance  $R_w$  from the centre of the profile to the axis of the workpiece rotation and the radius of the profile of the workpiece  $\rho_w$ . Thus, the radius-vector of the points of the screw surface, based on the general model (1) and the module of the workpiece (2), will be:

$$\bar{r}_w = S_{z_w \theta_w R_w \varphi_w \rho_w}^w \cdot e^{-4}, \quad (4)$$

$$S_{z_w \theta_w R_w \varphi_w \rho_w}^w = M_3(z_w(\theta_w)) M_6(\theta_w) \cdot M_2(R_w) \cdot M_4(\varphi_w) \cdot M_2(\pm \rho_w) \quad (5)$$

The radius of the profile  $\rho_w$  can take a positive and a negative value; a positive value indicates the screw surface of the screw and a negative value indicates the nuts. Model (4) can describe,

for example, the screw surfaces of the screw and the nuts of the ball screws.

2. Rotating surface with variable radius profile on the angle of rotation of the workpiece. Such a surface is characterized by the absence of the angular coordinate of the screw  $z_w$  and the constant distance  $R_w$  from the centre of the profile to the axis of the workpiece rotation. Thus, the radius vector of the points of rotation surface with a variable circular profile, based on the general model (1) and the module of the part (2), will be:

$$\bar{r}_w = S_{\theta_w R_w \varphi_w \gamma_p}^w \cdot e^{-4}, \quad (6)$$

$$S_{\theta_w R_w \varphi_w \gamma_p}^w = M_6(\theta_w) \cdot M_2(R_w) \cdot M_4(\varphi_w) \cdot M_2(\gamma_p) \quad (7)$$

Model (6) can describe, for example, the working surface of pipe rolls for the manufacture of seamless pipes. For such rolls, the parameters of the matrices  $\gamma_p$  and  $\varphi_w$  on the crimp section are functions of the independent parameter  $\theta_w$ . On the calibration section, where the profile becomes constant, they are converted to constants.

3. Concave torus surface. Such a surface is characterized by the absence of the angular coordinate of the screw  $z_w$ , the constancy of the distance  $R_w$  from the centre of the profile to the axis of the workpiece rotation and the radius of the profile of the torus surface  $\rho_w$ . Thus, the radius vector of the points of the rotation body of the concave torus surface, based on the general model (1) and the module of the part (2), will be:

$$\bar{r}_w = S_{\theta_w R_w \varphi_w \rho_w}^w \cdot e^{-4}, \quad (8)$$

$$S_{\theta_w R_w \varphi_w \rho_w}^w = M_6(\theta_w) \cdot M_2(R_w) \cdot M_4(\varphi_w) \cdot M_2(\pm \rho_w) \quad (9)$$

The radius of the profile  $\rho_w$  can take both positive and negative values. A positive value indicates an external concave torus surface and a negative value indicates an internal one. Model (8) can describe, for example, the grooves of the inner and outer bearing rings.

4. Convex torus surface. Such a surface is characterised by the absence of the angular coordinate of the screw  $z_w$ , the constancy of the distance  $R_w$  from the centre of the profile to the axis of the workpiece rotation and the radius of the profile of the torus surface  $\rho_w$ . Thus, the radius vector of the points of the rotation body with a convex torus surface, based on the general model (1) and the module of the part (2), will be:

$$\bar{r}_w = S_{\theta_w R_w \varphi_w \rho_w}^w \cdot e^{-4}, \quad (10)$$

$$S_{\theta_w R_w \varphi_w \rho_w}^w = M_6(\theta_w) \cdot M_2(R_w) \cdot M_4(-\varphi_w) \cdot M_2(-\rho_w) \quad (11)$$

From Fig. 1, we can infer that  $\varphi_w$  and  $\rho_w$  take negative values for the outer convex torus surface. Model (10) may describe, for example, roller saw blades, roll forming rollers, and belt pulleys.

### 3. GENERAL MODEL OF THE NOMINAL SURFACE OF THE TOOL

No matter which model describes the nominal surface of the workpiece, the tool radius vector in modular form is described by the transition matrix based on the workpiece shape.

$$\bar{r}_t = M_{tw} \cdot \bar{r}_w, \quad (12)$$

where  $M_{tw}$  – is the transition matrix from the coordinate system of the workpiece to the coordinate system of the tool. It describes the forming system of a machine tool that is involved in profiling the tool.

The matrix of transition (12) is the product of two spherical modules:

$$M_{tw} = S_{\theta_t \gamma_c}^{\varphi_t} \cdot S_{\psi}^o, \quad (13)$$

where:  $S_{\theta_t \gamma_c}^{\varphi_t}$  – is the module of the shape-building of a tool;  $S_{\psi}^o$  – is the module of the angular orientation of the tool relative to the details.

Shape-building module (13) consists of the product of two matrices:

$$S_{\theta_t \gamma_c}^{\varphi_t} = M_6(\theta_t) \cdot M_2(\gamma_c), \quad (14)$$

where:  $\theta_t$  – is the angle of rotation of the workpiece coordinate system relative to the axis of rotation of the tool;  $\gamma_c$  – is the distance between the axes of rotation of the tool and workpiece.

The module of orientation (13) is presented by the matrix of relative rotations:

$$S_{\psi}^o = M_5(\psi), \quad (15)$$

where:  $\psi$  – the angle of inclination of the grinding wheel.

The abrasive tool is editing on a constant surface (for example, on the calibration section of a tubular roll of variable radius profile); therefore only one variable parameter is used in module (15) – the angle of inclination of the wheel  $\psi$ .

To profile the tool, it is necessary to make an equation that determines the contact line, as follows:

$$\overline{V}_{tw} \cdot \overline{n}_w = 0, \quad (16)$$

where:  $\overline{n}_w$  – is the unit vector of normal line to the workpiece surface;  $\overline{V}_{tw}$  – is the vector of the velocity of the relative motion of the surface in the coordinate system of the tool.

The normal can be found as a vector product of vectors tangent to the surface. To find the normal, it is necessary to differentiate the radius vector of the workpiece surface by both angular parameters.

During the one-parametric rounding (Kalchenko et al., 2018) relationship between the parameters  $\varphi_w$  and  $\theta_w$  equal to zero of a mixed product of three vectors that are derived of the vector  $\bar{r}_t$ .

$$\left( \frac{\partial \bar{r}_t}{\partial \varphi_w} \times \frac{\partial \bar{r}_t}{\partial \theta_w} \right) \cdot \frac{\partial \bar{r}_t}{\partial \tau_w} = 0, \quad (17)$$

where:  $\left( \frac{\partial \bar{r}_t}{\partial \varphi_w} \times \frac{\partial \bar{r}_t}{\partial \theta_w} \right) = \overline{n}_w$  – is the vector normal to the surface of the workpiece at the point with curvilinear coordinates  $\varphi_w, \theta_w$ .  $\frac{\partial \bar{r}_t}{\partial \tau_w} = \overline{V}_w$  – is the vector of velocity of relative motion of the workpiece relative to the wheel;  $\tau_w$  – is the time of moving the workpiece, while turning it at the angle  $\theta_t$  in the opposite motion an axis  $O_t Z_t$  of the wheel.

The velocity of the workpiece regarding the wheel is determined by a matrix of transition from the workpiece coordinate system in the tool coordinate system:

$$\frac{\partial \bar{r}_t}{\partial \tau_w} = \frac{\partial M_6(\theta_t)}{\partial \theta_t} \cdot \frac{\partial \theta_t}{\partial \tau_w} \cdot M_{tw}, \quad (18)$$

where:  $\frac{\partial \theta_t}{\partial \tau_w} = \overline{\omega}_{tw}$  is the angular velocity of the workpiece rotation relative to the axis of the wheel.

We find the scalar product of vectors  $\overline{n_w}$  and  $\overline{V_{tw}}$  by writing down the determinant

$$\overline{V_{tw}} \cdot \overline{n_w} = \begin{vmatrix} X_{V_{tw}} & Y_{V_{tw}} & Z_{V_{tw}} \\ X_{\varphi_w} & Y_{\varphi_w} & Z_{\varphi_w} \\ X_{\theta_w} & Y_{\theta_w} & Z_{\theta_w} \end{vmatrix} = 0, \quad (19)$$

where  $X_{V_{tw}}, Y_{V_{tw}}, Z_{V_{tw}}$  – vector coordinates  $\overline{V_{tw}}$ ;  $X_{\varphi_w}, Y_{\varphi_w}, Z_{\varphi_w}$  – coordinates of the tangent  $\overline{A_w} = \frac{\partial \overline{r_t}}{\partial \varphi_w}$ ;  $X_{\theta_w}, Y_{\theta_w}, Z_{\theta_w}$  – coordinates of the tangent  $\overline{B_w} = \frac{\partial \overline{r_t}}{\partial \theta_w}$ .

The radius vector  $\overline{r_t}$  describes the plurality of tool surfaces. The choice of rational is made on the basis of the analysis of geometrical parameters of the outer surface of the workpiece and the allowance removal  $\delta$ .

#### 4. GENERAL MODEL OF THE REAL SURFACE OF THE TOOL AND WORKPIECE

Having determined the radius vector, we find that it is described by a spherical (torus) module, which is similar to the module of workpiece (1), but with own parameters, as follows:

$$\overline{r_t} = S_{\theta_t \cdot y_t \cdot \varphi_t \cdot y_p}^t \cdot e^{-4}, \quad (20)$$

$$S_{\theta_t \cdot y_t \cdot \varphi_t \cdot y_p}^t = M_6(\theta_t) \cdot M_2(y_t) \cdot M_4(\varphi_t) \cdot M_2(y_p) \quad (21)$$

where:  $\overline{r_t}$  – is the radius vector of the tool surface points;  $S_{\theta_t \cdot y_t \cdot \varphi_t \cdot y_p}^t$  – is the spherical module, that is a matrix of transition from the starting point to the coordinate system of the tool;  $\theta_t$  – is the angle of turning around the axis  $O_i Z_i$  of rotation of the tool;  $y_t = R_t$  – is the distance from the center of the profile of the tool to its axis of rotation;  $\varphi_t$  – is angle of rotation around the axis  $O_i Y_i$ ;  $y_p = \rho_t$  – is the radius wheel profile.

Creating a three-dimensional surface of the wheel is a very common way of learning the shaping processes (Uhlmann et al., 2016; Yan et al., 2011; Yanlong et al., 2013). Modelling in the MathCAD system allowed the determination of the maximum angle of the circle during processing (Fig. 2). Modelling was performed for the case of processing of constant trough profile  $Dw = 2Rw = 80$  mm, radius profile  $\rho_w = 20$  mm and central angle  $\xi = 140^\circ$ . Circle parameters: diameter 150 mm, height of circle 20 mm and ligament ceramic. As a result of the simulation, it was determined that for the selected conditions the contact line exists at  $\psi_t < 22^\circ$ . When the circle is tilted at  $22^\circ$ , the contact line disappears and contact occurs at the edges of the profile.

Thus, three spherical modules describe the radius vector of the workpiece surface:

$$\overline{r_{wt}} = S_{z_w \theta_w y}^\varphi \cdot S_{\varphi_t \psi_t x_t}^o \cdot \overline{r_t}, \quad (22)$$

where:  $S_{z_w \theta_w y}^\varphi = M_3(z_w) \cdot M_6(\theta_w) \cdot M_2(y_c + a \cdot \theta_w - \delta)$  – is the shaping module of details;  $\theta_w$  – is the angle of rotation coordinate system of the tool around the axis of rotation of the workpiece;  $y = y_c + a \cdot \theta_w - \delta$  – the current coordinate interaxial distance of the tool and workpieces;  $y_c$  – the distance between the axis of the wheel and the workpiece in the position of the residual molding of the workpiece surface;  $a = \frac{t}{2\pi}$  – is the constant of Archimedean spiral, which moves in relative motion wheel when removing of the allowance  $\delta$ ;  $S_{\varphi_t \psi_t x_t}^o = M_4(\varphi_t) \cdot$

$M_5(\pm \psi_t) \cdot M_1(x_t)$  – is the module of the angular orientation of the tool relative to the workpiece.



— 15 degree  
- - 20 degree  
- · - 21.9 degree

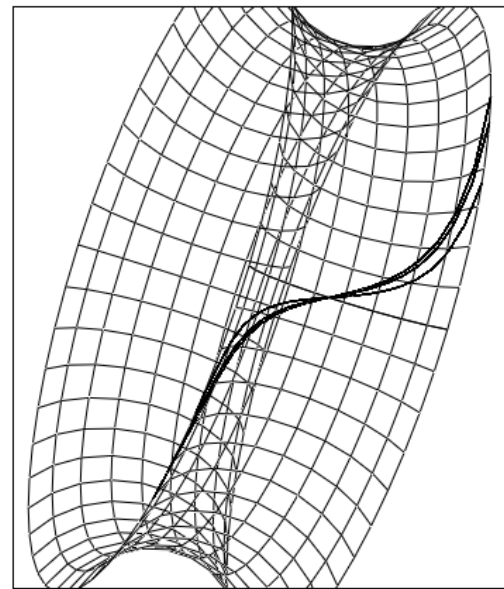


Fig. 2. The contact line of the wheel and the workpiece at different angles of a wheel

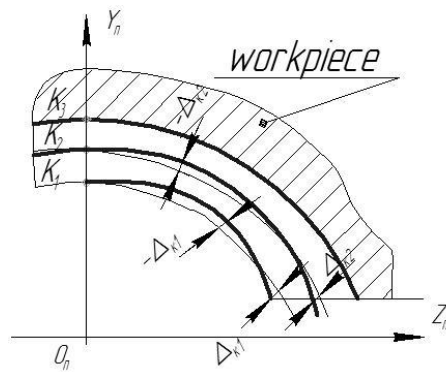


Fig. 3. The process of removing the allowance

When the allowance is removed,  $\delta = 0$  and  $y = y_c$ , the contact line which is rotating about the axis of the workpiece without

lateral movement describes the shape of the machined surface with radius  $\rho_w$ . Fig. 3 shows the allowance removal process. When inserting a wheel into the workpiece, we observe that at the same time its inclination will appear as errors ( $\Delta_{kj}$ , the value of which will decrease during the removal of the allowance. The final profile will be forming without error, since the wheel is straightening at the maximum angle of inclination at which the formation process is taking place. In this case, the radius of projection of the contact line of the wheel and the part on the axial plane will be equal to the radius of the groove profile  $\rho_w$ . The magnitude of the errors ( $\Delta_{kj}$  is determined by the least squares method and should not exceed the tolerances on the shape of the groove profile.

Model (22) describes a plurality of surfaces. To determine the real surface of the workpiece, it is necessary to make an equation describing the contact line.

$$\overline{V_{wt}} \cdot \overline{n_t} = 0, \quad (23)$$

where:  $\overline{n_t}$  – is the unit vector of normal line to the tool surface;  $\overline{V_{wt}}$  – is the vector of the velocity of the relative motion of the surface in the coordinate system of the workpiece.

By rotating the contact line around the axis of the workpiece with axial displacement  $z_w$ , we get a real contour of the workpiece surface.

### 5. GRINDING PROCESS WITH CROSSED AXES OF THE TOOL AND WORKPIECE

The method of processing workpiece with a profile in the form of an arc of a circle by the method of copying involves grinding by abrasive wheel, the height of which  $H^c$  is equal to the width  $B$  of the treated surface (Fig. 4). In this case, the radius of the wheel profile  $\rho_t^c$  is equal to the radius of the part profile  $\rho_p$  and, accordingly, greater than the radius of the workpiece profile  $\rho_w$ . When machining in this way, we removed just the variable allowance, because at the beginning of machining (pos. I) the wheel is cut by side sections of the profile and only at the end of machining (pos. II) the central point of the tool profile enters into the cutting process. At this time, the side sections of the wheel profile are not removed from the allowance, but create additional friction and increase the temperature in the cutting zone.

Grinding with the crossed axes of the tool and workpiece involves machining a narrow wheel, the height of which  $H$  is less than the width  $B$  of the work surface. The radius of the wheel profile  $\rho_t$  in the initial position is less than the radius of the part  $\rho_p$  and the radius of the workpiece profile  $\rho_w$ . The wheel is correction in an inclined position, the angle of inclination of which  $\psi_t$  corresponds to the maximum inclination of the wheel during processing, thereby achieving the equality of the radius of the contact line projection in the axial plane and the radius of the profile of the part  $\rho_p$ .

All parameters in figure 4 with index  $c$  – refer to the copy method. Parameters without index – the method of grinding with crossed axes.  $\rho_{te}$  and  $\rho_{te}^c$  – tool profile after editing for appropriate grinding methods.

One of the advantages of this method of processing over the traditional method of copying is the more efficient use of tool abrasives. In the traditional processing, the wear of the side part of the wheel by the value of  $k$  leads to the removal of a large part of the abrasive material  $F^c$  (Fig. 4). Since the centre angle of the tool profile in the proposed  $F^c$  is much less than the angle  $\xi^c$

in traditional method, the volume of abrasive  $F$  removed when editing a narrow wheel is much smaller (Fig. 4).

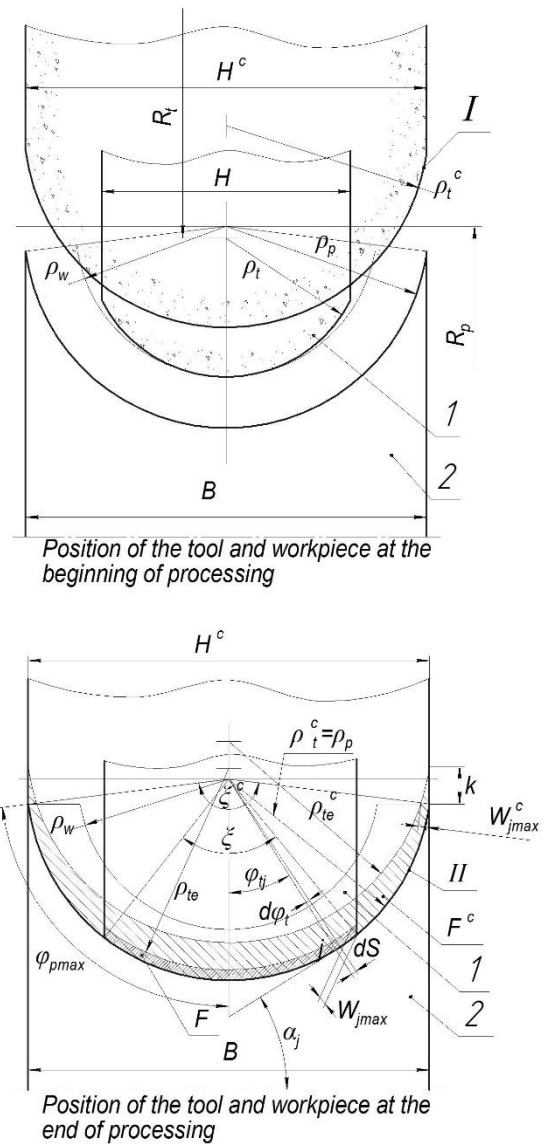


Fig. 4. Tool wear during machining

To restore the original shape of a circle in radius  $\rho_t^c$ , it is necessary to cut it in the direction perpendicular to the axis of rotation, by the value of  $k^c$ , which can be found from the relation (Kalchenko et al., 2020):

$$k^c = -(\rho_t^c - W_j) \cdot \sin \alpha_j + \sqrt{(\rho_t^c - W_j)^2 \cdot \sin^2 \alpha_j - W_j^2 + 2 \cdot \rho_t^c \cdot W_j} \quad (24)$$

The maximum wear  $W_{jmax}$  occurs at the  $j$ -th point of the wheel profile where  $\alpha_j = \varphi_{pmax}$ , on the side parts of the wheel profile. This causes frequent editing of the abrasive wheel with the removal of the abrasive array  $F^c$ . For example, with limited wear  $W_{jmax} = 0.05$  mm, it is necessary to cut a 3.16 mm of the wheel at the center point of the profile (Kalchenko et al., 2020). When editing a narrow wheel, it is necessary to remove the array  $F$ , which is much smaller.

To determine the limited wear of  $W_{jmax}$  for a narrow wheel, it is necessary to determine the performance of the grinding pro-

cess. The ways to solve of boundary-value problem discussed in detail in the works (Mikhailets V. 2015, 2018). The general model of removal of allowance and formation  $Q$  for machining surface of a workpiece with a circular profile, given in the form of a spherical module, has the form (Kalchenko et al., 2020):

$$Q = \int_0^T \left( \int_{-\varphi_{tmax}}^{+\varphi_{tmax}} \left( \int_{\theta_{1kj}}^{\theta_{2kj}} (\overline{V}_j \cdot \overline{n}_j - y_{sc}) \cdot (R_t + (\rho_t - W_j) \cdot \cos \varphi_{tj}) \cdot d\theta_k \right) \cdot \sqrt{\left( \frac{dR_{\varphi_{tj}}}{dj} \right)^2 + \left( \frac{d\varphi_{tj}}{dj} \right)^2} \cdot d\varphi_t \right) \cdot dT \quad (25)$$

where  $T$  – is the contact time of the part with the wheel;  $\pm \varphi_{tmax}$  – limit values of the angular position  $\varphi_{tj}$  of point  $j$  on the wheel profile;  $\theta_{1kj}$ ,  $\theta_{2kj}$  are the angular coordinates of a contact spot on a radius  $R_t + (\rho_t - W_j) \cdot \cos \varphi_{tj}$  (Fig.4);  $\overline{V}_j$ ,  $\overline{n}_j$  – vectors of cutting speed and normal at  $j$ -th point of a wheel;  $y_{sc} = f(\varphi_{tj}, K_{sc})$  – compliance of the processed system;  $K_{sc}$  – the value of static compliance;  $R_t$  – is the distance from the axis of rotation of the wheel to the center of its profile with radius  $\rho_t$ ;  $R_{\varphi_{tj}} = R_t + \rho_t \cdot \cos \varphi_{tj}$  – is the radius of rotation of the  $j$ -th point.

When moving from one cutting edge to an elementary part of the wheel  $dS$ , it is necessary to take into account the heterogeneity of the surface of the abrasive tool. It is possible to take into account the discontinuity of the surface of the wheel using the coefficient (Kalchenko et al., 2018):

$$\left[ 1 - \exp \left( - \frac{\sum_{i=1}^m b_t(t, \theta)}{b_0} \right) \right].$$

Model (25) describes the grinding performance for a single workpiece. To determine performance when processing a batch of workpieces  $Q$  must be multiplied at the number of workpieces in the batch.

The general 3D model (25) of the allowance removal and the formation makes it possible to determine the local productivity  $Q_l$  at each elementary section  $dS$  (Fig. 4) of the contact spot  $S$  of wheel 1 and workpiece 2. In model (25)  $R_t + (\rho_t - W_j) \cdot \cos \varphi_{tj} \cdot d\theta_k$  – the length of the elementary section is measured along the arc of a circle with radius  $R_t + (\rho_t - W_j) \cdot \cos \varphi_{tj}$ . The width of the elementary section in the axial section of the

circle is determined by the differential  $\sqrt{\left( \frac{dR_{\varphi_{tj}}}{dj} \right)^2 + \left( \frac{d\varphi_{tj}}{dj} \right)^2}$ .

The specific productivity  $Q_{sj}$  is determined by the internal integral of the model (25). It shows how much metal is cut by a wheel within the  $j$ -th point of the profile.

The instantaneous grinding performance  $Q_i$  is described by the surface integral of model (25). It allows the determination of the instantaneous volume of metal that cuts into the contact spot of the wheel and the workpiece.

The average grinding performance  $Q_a$  is determined by the ratio:

$$Q_a \text{ is determined by the ratio:} \quad Q_a = \frac{Q \cdot n}{t} \quad (26)$$

where  $Q \cdot n$  – is the volume of metal removed from  $n$  parts over time  $t$ .

The analysis of model (25) shows that when  $\overline{V}_j \cdot \overline{n}_j > 0$  the allowance is removed from the workpiece. This takes place when  $\overline{V}_j \cdot \overline{n}_j = 0$  metal is not cutting and we have the process of form-

ing the surface of the workpiece  $\overline{r}_{pi}$ . Productivity increases with the increase of scalar product vectors  $\overline{V}_j \cdot \overline{n}_j$  and the rigidity of the machined system, the contact area  $S$  of the wheel and the details of the processing coordinate, the angle  $\psi_t$  and the decrease in the wear profile  $W_j$  of the wheel (Mamalis et al., 2016; Grabchenko et al., 2014; Shakhbazov et al., 2019).

The amount of worn abrasive per unit time is calculated for the section of the wheel profile  $dS$  from equation (Mamalis et al., 2016; Grabchenko et al., 2014)

$$Q_a = k_\alpha \cdot 2\pi \cdot (R_t + \rho_t \cdot \cos \varphi_{tj}) \cdot J_j, \quad (27)$$

where  $J_j$  – abrasive wear at a certain grinding speed in the direction normal to the tool profile per unit time;  $k_\alpha$  – is the coefficient that takes into account the overlapping of the cutting edges.

The value of the elemental wear rate of a circle  $J_j$  over time  $dt$  has the form

$$J_j = \frac{C_{sj} \cdot Q_{sj}^{m_j} + C_{dj} \cdot Q_{dj}^{b_j}}{k_\alpha \cdot 2\pi \cdot R_{\varphi_{tj}}} \quad (28)$$

where  $C_{sj}$ ,  $C_{dj}$  – are the coefficients of specific wear at the  $j$ -th point of the wheel profile at  $Q_{sj} = 1$  and  $Q_{dj} = 1$ , which are determined experimentally for each  $j$ -th point of the wheel profile;  $Q_{sj}$  – the specific volume of the metal being removed by the  $j$ -th point of the wheel profile, determined from the expression (25) at  $\overline{V}_j \cdot \overline{n}_j \cdot \tau_j \geq a_{zmin}$ ;  $\tau_j$  – the time between the contacts of the cutting grains;  $a_{zmin}$  – the minimum thickness of the layer which cut off by the cutting edge;  $Q_{dj}$  – the specific volume of metal deformed by abrasive grains of the  $j$ -th point of the wheel profile, determined from expression (25) at  $\overline{V}_j \cdot \overline{n}_j \cdot \tau_j \leq a_{zmin}$ ;  $m_j$  – the coefficient that takes into account the intensity of the grinding mode and the state of the cutting surface of the wheel; and  $b_j$  – the coefficient that takes into account the intensity of the deformation mode of the metal without its removal.

The linear wear of  $W_j$  at the  $j$ -th point of the wheel profile during the machining process is determined by the equation (Mamalis et al., 2016; Grabchenko et al., 2014)

$$W_j = \int_0^{T_0} \frac{C_{sj} \cdot Q_{sj}^{m_j} + C_{dj} \cdot Q_{dj}^{b_j}}{k_\alpha \cdot 2\pi \cdot (R_t + \rho_t \cdot \cos \varphi_{tj})} dT_0 \quad (29)$$

where  $T_0$  – is the processing time of the workpiece for part of its rotation, one revolution or the number of revolutions required to process the workpiece by a section of a wheel within the  $j$ -th point of its profile.

## 6. CONCLUSIONS

The general model was developed and on its basis special models of process of grinding with the crossed axes of the tool and workpiece with a profile in the form of a circle arc were formulated.

A new method of control of the grinding process is proposed, which will provide processing by equidistant curves, and the value of cutting of a wheel equal to the allowance. This will increase the productivity and quality of grinding. Based on the developed method, it is necessary to develop a package of applications that would allow programming of CNC machine tools by programmers

who do not have special training.

The presented method of grinding implements the processing with the spatial contact line of the tool and workpiece. When the axes are crossed, the contact line is stretched, which leads to an increase of the contact area and, accordingly, to decrease of the temperature in the processing area. This allows processing of the workpiece with more efficient cutting modes. The developed mathematical models are the basis for experimental research.

## REFERENCES

1. **Anderson D., Warkentin A., Bauer R.** (2011), Experimental and numerical investigations of single abrasive-grain cutting, *International Journal of Machine Tools & Manufacture*, 51, 898-910.
2. **Chi Y., Li H.** (2012), Simulation and analysis of grinding wheel based on Gaussian mixture model, *Frontiers of Mechanical Engineering*, 7(4), 427-432.
3. **Cong S., Yansheng D., Dongxue L., Shichao X.** (2018), Modeling and predicting ground surface topography on grinding chatter, *Procedia CIRP*, 71, 364-369.
4. **Grabchenko A., Fedorovich V., Pyzhov I., Kunderák J.** (2014), 3D simulation of vibrating diamond grinding. *Manufacturing Technology*, 14(2), p. 153-160.
5. **Kacalak W., Lipiński D., Szafraniec F., Tandecka K.** (2018), The methodology of the grinding wheel active surface evaluation in the aspect of their machining potential, *Mechanik*, 91 (8-9), 690-697.
6. **Kacalak W., Szafraniec F., Lipiński D.** (2018), Methods for modeling the active surface of grinding wheels, *Mechanik*, 91 (10), 907-914.
7. **Kalchenko V., Kalchenko V., Sira N., Yeroshenko A., Kalchenko D.** (2020) Three-Dimensional Simulation of Machined, Tool Surfaces and Shaping Process with Two-Side Grinding of Cylindrical Parts Ends. In: Tonkonogyi V. et al. (eds) *Advanced Manufacturing Processes. InterPartner 2019*. Lecture Notes in Mechanical Engineering. Springer, Cham, 2020, p. 118-127.
8. **Kalchenko V., Yeroshenko A., Boyko S.** (2018), Crossing axes of work-piece and tool at grind-ing of the circular trough with variable profile, *Acta Mechanica et Automatica*, 12(4),281-285.
9. **Kalpana K., Arunachalam N.** (2018), Grinding wheel redress life estimation using force and surface texture analysis. *Procedia CIRP*, 72, 1439-1444.
10. **Mamalis A.G., Grabchenko A.I., Fedorovich V.A., Romashov D.V.** (2016), Improving the design of diamond wheel for high-speed grinding. *Journal of Machining and Forming Technologies*. Nova Science Publishers, Inc. Volume 8, Number 1-2, 12 p.
11. **Mikhailiets V.A., Chekhanova G.A.** (2015), Limit theorems for general one-dimensional boundary-value problems. *Journal of Mathematical Sciences*, Vol. 204, No. 3, p. 333-342.
12. **Mikhailiets V.A., Pelekhat O.B.** (2018), Limit theorems for the solutions of boundary-value problems. *Ukrainian Mathematical Journal*, Vol. 70, p. 216-223.
13. **Shakhbazov Y., Shyrokov V., Fedorovych V.** (2019), Specifying the Process Parameters for Diamond Dressing of Grinding Wheels. *Journal of Superhard Materials*, Volume 41, p. 272-277.
14. **Uhlmann E., Koprowski S., Weingaertner W.L., Rolon D.A.** (2016), Modelling and Simulation of Grinding Processes with Mounted Points: Part II of II - Fast Modelling Method for Workpiece Surface Prediction. *Procedia CIRP*, 46, 603-606.
15. **Yan L., Rong Y.M., Jiang F., Zhou Z.X.** (2011), Three-dimension surface characterization of grinding wheel using white light interferometer. *International Journal of Advanced Manufacturing Technology*, 55, 133-141.
16. **Yanlong C., Jiayan G., Bo L., Xiaolong C., Jiangxin Y., Chunbiao G.** (2013), Modeling and simulation of grinding surface topography considering wheel vibration. *The International Journal of Advanced Manufacturing Technology*, 66(5-8), 937-945.